ELSEVIER

Biochimica et Biophysica Acta 1459 (2000) 440–448

BIOCHIMICA ET BIOPHYSICA ACTA
BBA

www.elsevier.com/locate/bba

Crystallographic location of two Zn^{2+}-binding sites in the avian cytochrome bc_1 complex

Edward A. Berry [a,*], Zhaolei Zhang [b], Henry D. Bellamy [c], Lishar Huang [a]

[a] *Lawrence Berkeley National Laboratory, University of California, Berkeley, CA, USA*
[b] *The Graduate Group of Biophysics, University of California, Berkeley, CA, USA*
[c] *Stanford Synchrotron Radiation Laboratory, Stanford, CA, USA*

Abstract

The chicken mitochondrial ubiquinol cytochrome *c* oxidoreductase (bc_1 complex) is inhibited by Zn^{2+} ions, but with higher K_i (~ 3 μM) than the corresponding bovine enzyme. When equilibrated with mother liquor containing 200 μM $ZnCl_2$ for 7 days, the crystalline chicken bc_1 complex specifically binds Zn^{2+} at 4 sites representing two sites on each monomer in the dimer. These two sites are close to the stigmatellin-binding site, taken to be center Q_o of the Q-cycle mechanism, and are candidates for the inhibitory site. One binding site is actually in the hydrophobic channel between the Q_o site and the bulk lipid phase, and may interfere with quinone binding. The other is in a hydrophilic area between cytochromes *b* and c_1, and might interfere with the egress of protons from the Q_o site to the intermembrane aqueous medium. No zinc was bound near the putative proteolytic active site of subunits 1 and 2 (homologous to mitochondrial processing peptidase) under these conditions.

1. Introduction

Specific, high-affinity organic inhibitors have played a major role in defining the pathways of electrons through the mitochondrial cytochrome bc_1 complex [1]. Inhibition of respiration by a number of heavy metals, including Zn^{2+}, has been studied by Skulachev and coworkers [2]. Papa and co-workers further investigated binding and inhibition by zinc [3], and showed that zinc was bound to the Rieske iron-sulfur protein (ISP) after isolating the individual subunits by SDS–PAGE.

Link and von Jagow [4] showed that the high-affinity binding site was still present after removal of the ISP subunit. They showed that inhibition by zinc was noncompetitive with respect to quinol and cytochrome *c* but was pH dependent; i.e., competitive with H^+ ion, a substrate and product of this proton-translocating electron transfer enzyme. They proposed that zinc inhibits by interfering with a proton pathway linking the quinol oxidizing (Q_p or Q_o) site to the intermembrane space where protons are deposited by turnover of the enzyme.

Rao et al. [5] studied inhibition of the chloroplast cytochrome b_6f complex by Cu^{2+} ions. The characteristics were somewhat different, with inhibition being competitive with respect to plastoquinol and with a different pH dependence. They concluded that the inhibitory Cu^{2+}-binding site was some distance from the Q_o site, and proposed a histidine residue in cytochrome *f* as a likely ligand.

The two largest subunits of the mitochondrial bc_1 complex, chains A and B, are homologous to the β and α subunits of the matrix processing protease (MPP) [6,7] involved in cleavage of the signal se-

* Corresponding author. Physical Biosciences Division, Melvin Calvin Laboratory, 1 Cyclotron Road, MS 3-250J, Berkeley, CA 94720, USA. Fax: +1-510-486-6059;
E-mail: eaberry@lbl.gov

0005-2728/00/$ – see front matter
PII: S0005-2728(00)00182-1

quence after import of cytoplasmically transcribed proteins into the mitochondrion. In yeast and mammalian mitochondria MPP is a soluble matrix protein, a Zn protease of the insulinase family with a conserved Zn-binding site in the β-subunits [8,9]. In plants this Zn-binding site is conserved in the bc_1 complex subunit 1, and the isolated bc_1 complex has processing protease activity that is inhibited by chelating agents [10]. In the vertebrate bc_1 complex the Zn-binding site can be identified by alignment; however, it has been altered by mutation of one histidine to tyrosine, and it is not clear whether it would bind zinc tightly. Nevertheless some metal-ion-dependent protease activity has been demonstrated after partial denaturation of the bovine bc_1 complex by detergent [11].

Recently several groups have determined the structure of the vertebrate bc_1 complex by crystallization and X-ray diffraction [12–14]. In this work we report that the chicken bc_1 complex is also inhibited by Zn^{2+} but with a lower affinity than the bovine enzyme. We define zinc-binding sites in the crystalline chicken bc_1 complex by analysis of X-ray data from crystals treated with Zn^{2+} at sub-millimolar concentration for 1 week. The data were collected at an X-ray wavelength which maximized the anomalous signal from zinc.

2. Materials and methods

The decyl analog of ubiquinone (2,3 dimethoxy-6-decyl-1,4-benzoquinone) was purchased from Sigma Chemical Co. and reduced to the quinol (DBH) as described in [15]. Quinol:cytochrome *c* oxidoreductase was measured as in [15] except that KCN and EDTA were omitted from the reaction mixture, which contained 40 mM KP_i (pH 7.5), 40 μM horse heart cytochrome *c*, and 0.05 g/l dodecyl maltoside. Up to 10 μl $ZnCl_2$ was added to 1 ml reaction mix, from a stock solution of 0.1, 1, 10, or 100 mM, to give the desired concentration. About 10 pmol of bc_1 complex was then added and incubated for 1 min before starting the reaction by addition of 2 μl of 25 mM ethanolic DBH. Absorbance change at 550–535 nm ($\Delta\Delta\varepsilon_{mM} = 25$) was followed for 15 s and activity was calculated from the average slope from 1 s to 15 s or wherever the trace went offscale. Rates from the tangent at 1 s were higher but less reproducible.

Crystals were grown and cryoprotected as described [13]. Two months after setting up the crystallization tray, a few crystals were transferred to a droplet containing 25 μl of the mother liquor supplemented with glycerol and 1 μl of 5 mM $ZnCl_2$, for a total Zn^{2+} concentration just under 200 μM. As some of this was bound by the protein, the actual free concentration was lower, probably between 100 and 200 μM. After equilibration for 7 days a crystal was removed from the soaking solution and frozen in liquid nitrogen. Data were collected at SSRL's beamline 1–5, using a Quantum4 CCD detector at a distance of 200 mm from the crystal. The X-ray energy was tuned to the Zn K absorption edge at 9660 eV (1.283 Å) to maximize the Bijvoet differences. Completeness and R_{sym} statistics for the data are given in Table 1. Initial model refinement (rigid-body, Powell minimization, and individual atomic B-factor) in CNS was carried out using all reflections in the range 25–3.7 Å, with no sigma cutoff. This gave a total of 72139 reflections, corresponding to 89.5% completeness over that range and giving an effective resolution of 3.85 Å. Of these 72139 reflections 5%, or 4.5% of a complete 3.7 Å set, were reserved for the test set to calculate the R_{free} value. All model refinement was done using the CNS program [16], version 0.1.

Table 1
Diffraction data statistics

Space group	$P2_12_12_1$
Cell dimensions	171.4 181.2 241.1
Resolution	3.48
Effective resol.	3.65
Observations	344595
Unique refl.	84122
Completeness	86% (44%[a])
$I/\sigma I$	19.1 (1.3)
R_{sym}	0.179 (0.99)

Values in parentheses refer to the highest resolution shell, 3.48–3.54 Å.
[a]Low completeness in last shell is due to overlap, not to rejected weak reflections. No σ cutoff was used.

3. Results and discussion

3.1. Inhibition of quinol:cytochrome c oxidoreductase activity by Zn^{2+}

The pattern of inhibition of chicken bc_1 complex by $ZnCl_2$ is somewhat different than that of the bovine enzyme. (Fig. 1). The activity is reduced to about 30 s^{-1} with a K_i around 3 μM, but that residual activity (about 20%) is not further reduced even at 200 μM. This residual activity is inhibited by myxothiazole (Solid square in Fig. 1). Experiments under similar conditions with the bovine bc_1 complex confirmed the higher-affinity inhibition of this enzyme ($K_i \sim 0.1$ μM) reported by Link et al. [4]. The pH dependence was not investigated. Zn inhibition of the chicken enzyme was similar when the quinol concentration was reduced 10-fold, suggesting the inhibition is not significantly competitive with the quinol substrate.

3.2. Structure factor phase determination

As described in Section 2, a diffraction dataset was collected near the Zn absorption edge for a crystal of avian bc_1 complex soaked with 0.2 mM $ZnCl_2$ for 7 days. The dataset was phased using a model of the native bc_1 structure, based on the PDB model 1BCC but further refined against a dataset obtained by merging our seven best datasets from this crystal form. This structure was located in the Zn-containing crystal by rigid body rotation using the program CNS. First the entire dimer was treated as one rigid body, then the individual subunits and hetero groups were each treated as rigid bodies. The transmembrane and extrinsic domains of the Rieske iron–sulfur protein were treated as two separate rigid bodies.

The resulting structure, with anisotropic B-factor scaling and bulk solvent correction, had an R value of 0.315 and R_{free} of 0.322 over the resolution range 25–3.7 Å. The model, still without any Zn ions, was then subjected to 60 steps of atomic positional refinement and 30 steps of atomic B-factor refinement, minimizing a maximum-likelihood target on amplitudes (mlf). This improved R and R_{free} slightly, to 0.289 and 0.317. The structure is similar to the native structure (PDB entry 1BCC), with the extrinsic domain of the Rieske ISP and the side chain of Glu272 (cytochrome b) in the same position as in that structure with empty Q_o site, and not in the positions

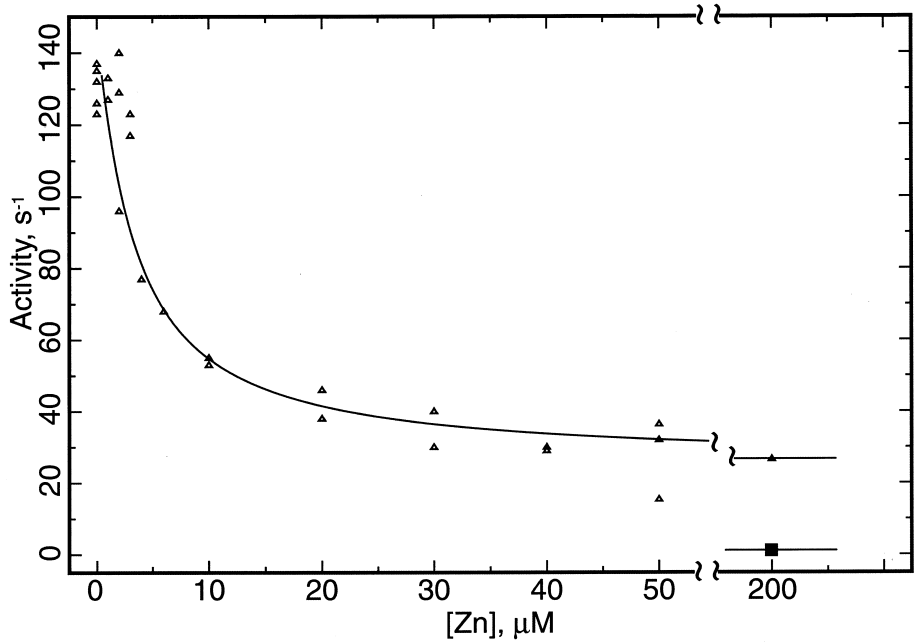

Fig. 1. Inhibition of the ubiquinol:cytochrome c reductase activity of purified chicken bc_1 complex by $ZnCl_2$. Electron transfer from the decyl analog of ubiquinone to horse heart cytochrome c was assayed as described in materials and methods. Open triangles, inhibition by $ZnCl_2$ alone. Solid square, inhibition by 2 μM myxothiazole as well as 200 μM $ZnCl_2$.

induced by binding stigmatellin (3BCC) or (presumably) ubiquinol. The ordering of the ISP extrinsic domain was unusually poor, however, and it is impossible to say if there were changes there.

3.3. Location of bound Zn ions in the crystal

Structure factors were calculated for the refined Zn-free model and the observed amplitudes were scaled against the calculated ones to approximate an absolute scale, using the CCP4 programs SFALL and RSTATS. A Bijvoet difference Fourier map was calculated with coefficients of F^+–F^- and phases Φ_c retarded by 90°. The resulting map ranged in density from −0.141 to 0.180 with RMS deviation from mean (σ) of 0.0255. An omit map (with coefficients of F_o–F_c) was also calculated. Its density ranged from −0.520 to 0.892, with σ 0.0853.

Density peaks within one asymmetric unit were picked from both maps. The anomalous (Bijvoet difference) map yielded 19 peaks with amplitude greater than 4.5σ which were further analyzed as potential bound Zn sites. A cutoff of 4.0 s was used for the omit map, yielding 134 peaks. Properties of the peaks that were further analyzed are listed in Table 2.

Three of the anomalous peaks were in the vicinity of heme Fe atoms and were attributed to anomalous scattering of the iron, which has an F'' value of 2.37 e^- at this wavelength, compared with approximately 3.9 e^- for Zn. If the threshold was lowered then anomalous peaks for all six heme irons were observed at 3.8–6.0σ. Surprisingly, these iron peak positions were as much as 1.5 Å from the refined positions of the irons, suggesting a possible need for improvement in the heme parameter files used in refinement. No anomalous signal from the Rieske Fe_2S_2 cluster was observed using a 3.5 s cutoff, and in fact an omit map for the Rieske protein showed no strong peak where the iron was expected, suggesting the cluster is lost or the protein is deranged in some way after a week's exposure to $ZnCl_2$.

Of the 19 peaks greater than 4.5σ in the anomalous map, five were within 1 Å of a peak above 4σ in the omit map and thus were candidates for a bound Zn position. As can be seen in Table 2, one of these could be attributed to the heme iron of cytochrome c_1, and was not considered further. The other four, including the three strongest and the seventh strongest anomalous peaks, did not correspond to any Fe position and were related by NCS symmetry. After examination of the binding regions (described below) these were assigned to two Zn ions in each monomer.

Table 2
Peak heights and spatial separation of peaks in the anomalous and omit (F_o–F_c) maps

Assignment[a]	Peak height: σ (rank)		Peak discrepancy (Å)[b]		Atomic B[c]
	ano	omit	ano–omit	ano–M[c]	
Zn01A	7.17 (1)	4.87 (27)	0.4	0.7	111.0
Zn01B	5.20 (7)	4.61 (48)	0.8	1.1	112.0
Zn02A	6.54 (3)	10.75 (1)	0.5	0.6	25.0
Zn02B	6.58 (2)	10.07 (2)	0.5	0.9	53.0
Fe1A	4.46 (28)			0.4	42.5
Fe2A	6.03 (4)			0.8	37.3
Fe3A	4.57 (20)	5.03 (19)	0.6	1.5	55.7
Fe1B	5.55 (5)			0.7	48.1
Fe2B	4.21 (72)			1.2	45.6
Fe3B	3.80 (282)			0.8	57.4

[a]Fe1, 2, and 3 are the Fe atoms of heme b_L, heme b_H, and cytochrome c_1. Zn01 and Zn02 are the two zinc ions located in this study. A and B refer to the two monomers in the asymmetric unit.

[b]For each site, the discrepancy (distance) between the peak in the anomalous map and either the peak in the omit map (column 4) or the refined position of the metal ion (column 5).

[c]For iron atoms the values (atomic position or B-factor) were taken from the refined model without zinc that was used to phase the anomalous and F_o–F_c maps. For the Zn ions, the values were taken after further positional and atomic B-factor refinement with the four Zn ions added to the model at the positions of the anomalous peaks (i.e., this information was not used in positioning the zincs, but in evaluating the final model).

The zinc ions (Zn01 and Zn02) were added to the model and refinement continued. No significant decrease in the *R*-factor was observed, as might be expected considering that the Zn ions constitute only 130 Da out of 240 kDa for the protein and that several phospholipid molecules have not yet been modeled. At this point the resolution was extended to 3.5 Å. The refined positions were used to identify likely ligands (next section), and 'patches' representing bonds (between Zn01 and side chains of D253, E255, H268 in cytochrome *b* and H121 in cytochrome c_1; and between Zn02 and M125) were used for further refinement. The resulting structure was used to make the diagrams of the binding sites shown in Figs. 2 and 3. The final refined model had *R*-factor and R_{free} of 0.290 and 0.319 to 3.5 Å.

3.4. Description of the Zn-binding sites

To look at potential ligands and van der Waals contacts of zinc in the sites identified, we made a list (Table 3) of all protein atoms within 3.8 Å of the Zn ions after preliminary positional refinement (with the Zn ions in the model, but without defining bonded interactions). Zn01 is in a hydrophilic area between cytochromes *b* and c_1, with potential ligands from both proteins. These include His121 in cytochrome c_1 and Asp253 in the de linker loop of cytochrome *b*. Glu255 (cytochrome *b*) is another possible ligand. H268 of cytochrome *b* is also in the vicinity but did not refine into a coordinating position. Electron density for the side chain of this residue was poor, and the refined B-factors were high ($\sim$100). When the Zn ions were added and refinement continued assuming ligation to all four of these residues ('patches' were used in CNS), a reasonable coordination geometry was obtained (Fig. 2); however, from the present data we cannot confirm involvement of H268 or E255 in coordination of Zn01.

Zn02 is in a hydrophobic area in the channel between the Q_o quinol-binding site in cytochrome *b* and the bulk lipid phase. If the Zn-crystal structure is superimposed on the structure with stigmatellin bound (Figs. 2 and 3), Zn02 is overlapping the hydrophobic 'tail' of stigmatellin about four carbons from the ring, at the level of the first side chain methoxy group. The only electronegative protein atom in the vicinity of Zn02 is Sδ of Met125 of cytochrome *b*. We have been unable to find any examples of Zn bound to a methionine S atom in the

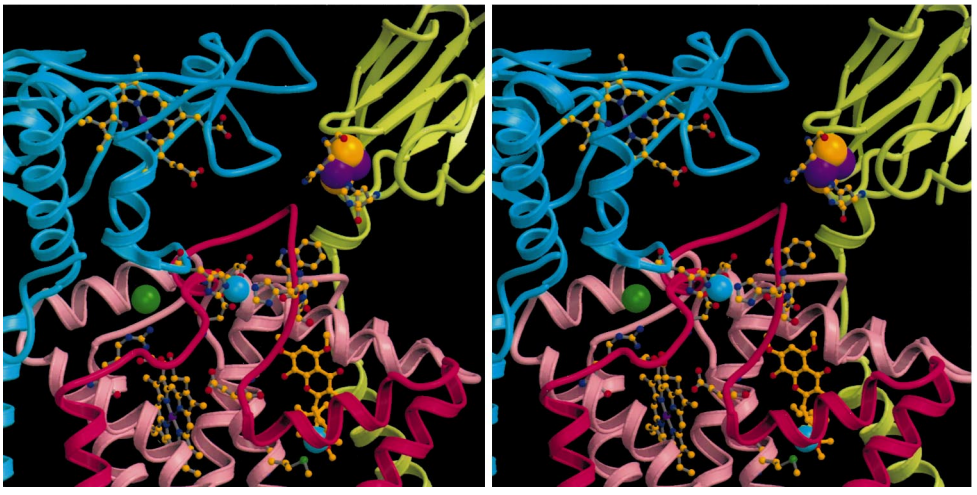

Fig. 2. Stereo view of Zn01 in its binding site. The site of Zn01 (cyan sphere near center) is in the interface between cytochrome *b* (salmon), cytochrome c_1 (blue), and the ISP (green) The ef linker of cytochrome *b*, which provides three of the four potential ligands for Zn01, is highlighted with a darker shade. The yellow and red ball-and-stick model to the right and below Zn01 is stigmatellin from the superimposed 3BCC structure (see legend to Fig. 3). Glu272 is visible between stigmatellin and the low potential heme of cytochrome *b*. The green sphere to the left and behind Zn01, shown bonded to R81 of cytochrome *b*, is the density mentioned in the text that is present in all crystals, independent of $ZnCl_2$ treatment, and is modeled as a Cl^- ion. Zn02 is also visible, partially obscured by the horizontal ef helix. M125 is shown as a ball-and-stick model below and to the left of Zn02. The figure was made with Molscript [21] and Raster3D [22].

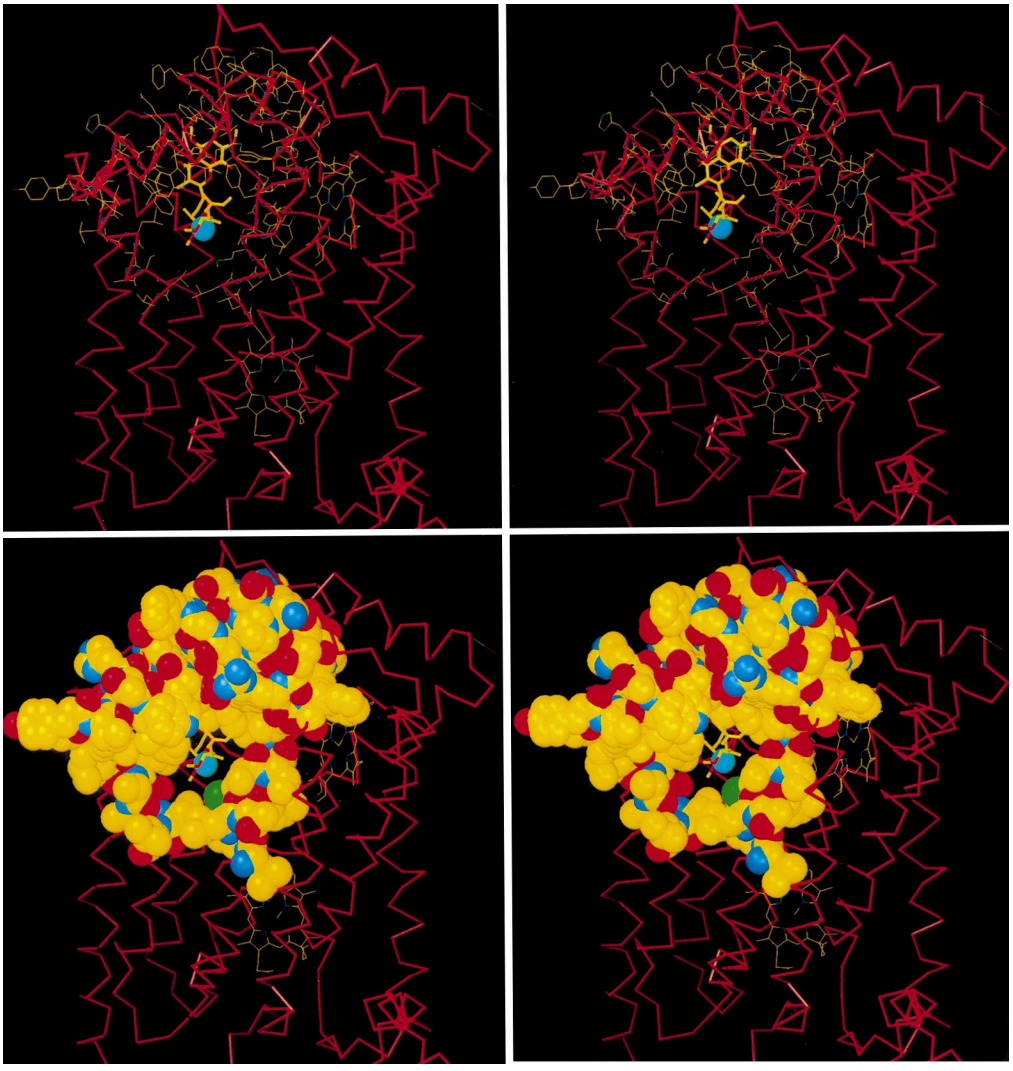

Fig. 3. View of Zn02 binding in the hydrophobic channel between the Q_o site and the bulk lipid phase. Stereo view of the cytochrome *b* backbone (red Ca trace) with the residues around the channel portrayed as wireframe (above) and space-filling (below) models, viewed from the position of the second cytochrome *b* monomer. Stigmatellin is the thick yellow and red stick model, with the hydrophobic tail pointed toward the viewer. (The orientation is related to that of Fig. 2 by approximately 180° rotation about the vertical axis.) When viewed in stereo the residues depicted are seen to form a channel around the hydrophobic tail of stigmatellin. The cyan sphere in the middle of the channel, through which the stigmatellin passes, represents the position of Zn02. The green sphere in the wall of the channel in the space-filling model is Sd of MET125, the protein atom most closely associated with the zinc. The stigmatellin coordinates are from an updated version of the coordinates deposited as 3BCC. The zinc is from the current structure. Both coordinate sets were transformed to a standard reference cell in order to superimpose structures from slightly different cells. The figure was made using the graphics program O [23].

protein database, and the distance is approximately 3.5 Å instead of 2.2–2.35 which is typical for Zn–S bonds in zinc ligated by cysteine [17]. Nonetheless, the electron density of Zn and the side chain are very strongly connected, being continuous when contoured at up to 4.5 sigma in a $2F_o$–F_c map calculated from phases from the model containing Zn.

3.5. A new heavy atom site in the native bc_1 complex

Electron density maps for all of our chicken bc_1 crystals show strong density apparently attached to the guanidino group of R81 in cytochrome *b*. If we modeled it with a water molecule at full occupancy, the B-factor refined to a value much lower than the

Table 3
Potential ligands for the Zn ions

Metal ion	Ligand/contact			Distance (Å)	Ligand/contact			Distance (Å)
	Residue	Type	Atom		Residue	Type	Atom	
Zn01	C253	Asp	Cγ	3.5	P253	Asp	Cγ	3.9
	C253	Asp	Oδ1	3.6	P253	Asp	Oδ1	3.9
	C253	Asp	Oδ2	2.7	P253	Asp	Oδ2	3
	C255	Glu	Oε1	3.7	P255	Glu	Oε1	3.5
	C268	His	Cβ	3.9	P268	His	Cβ	3.6
					P268	His	Nδ1	3.9
					P268	His	O	3.8
	D121	His	Cδ2	3.9				
	D121	His	Cε1	3.6	Q121	His	Cε1	3.3
	D121	His	Nε2	2.9	Q121	His	Nε2	3
Zn02	C125	Met	Sδ	3.3	P125	Met	Sδ	3.6
	C275	Phe	Cδ1	3.8	P275	Phe	Cδ1	3.9
	C275	Phe	Cε1	3.3	P275	Phe	Cε1	3.4

Distances from the refined Zn positions to the nearest neighboring atoms after refinement with the Zn ions but without patches defining the ligands.

surrounding atoms. This suggests the scattering power is much greater than that of a water molecule. Replacing it with a Cl^- still gave quite low B-factors (14 and 33). Positional refinement of the Cl without patch parameters gave N–Cl distances of 3.5 and 4.0 in the two monomers. Another possible interpretation of this density is the phosphate head group of a phospholipid whose side chains are too disordered to visualize.

This density was modeled as Cl^- in the updated 1BCC coordinates used to phase the Zn crystal dataset. At the time the patches for Zn atoms were incorporated a patch for the Cl atom was also incorporated, specifying a bond of 3 Å. In the final refined model the B-factors were 24 and 45, lower than the main-chain atoms of R81. The positions of this atom and R81 are shown in Fig. 2.

3.6. No Zn^{2+} binding at the modified inverse zinc-binding motif of subunit 1

Fig. 4 shows an alignment of mammalian bc1 complex subunit 1 (core I) with various eukaryotic MPP β subunits in the region of the 'inverted zinc-binding motif' [8], corresponding to 101:HXXEHX_{68}E in the rat liver β-MPP. Note

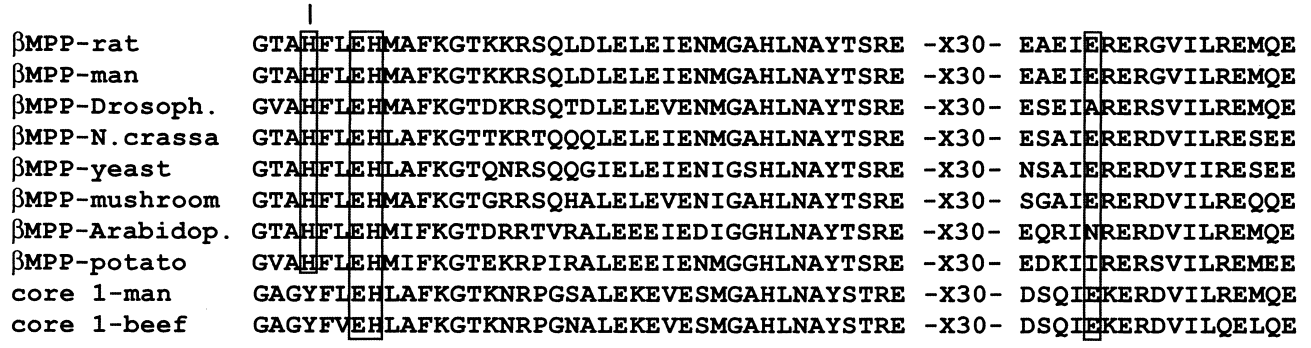

Fig. 4. Alignment of vertebrate bc_1 complex subunit one with the inverse zinc-binding motif of β-MPP. Residues making up the motif, (HXXEH-Xn-E), are boxed. The histidine which is mutated to Y in core 1 protein is indicated by a vertical mark above the first row. In some cases, notably *Neurospora* and potato, β-MPP is subunit 1 of the bc_1 complex.

that the β-MPP subunit is in fact subunit 1 of the bc_1 complex in the potato and *Neurospora* enzymes. We do not have the sequence of the chicken core 1 protein, but assume it is similar to the bovine protein. In the mammalian core I protein the first histidine in the motif has been replaced by tyrosine (Y101), making it uncertain whether the site binds Zn^{2+} with high affinity. As mentioned before, the only strong peaks coinciding in both maps belong to the two Zn sites identified above and one heme iron. We looked for anomalous or difference map peaks in subunit 1 in the zinc-soaked crystal. No anomalous or omit peak above 3.5σ was within 5 Å of the residues E60 or H61, suggesting they do not form a high-affinity zinc-binding site in the chicken bc_1 complex.

4. Conclusions

Like the bovine cytochrome bc_1 complex, the avian complex is inhibited by Zn^{2+} ions. Inhibition appears to be noncompetitive with respect to the quinol substrate, as with the bovine complex. However, inhibition is incomplete in the case of chicken complex, with a residual turnover around 30 s^{-1} in the presence of saturating Zn^{2+} concentration. Also this incomplete inhibition titrates with a higher K_i.

It is tempting to speculate that the Zn01 site between cytochrome *b* and cytochrome c_1 is the site characterized by Link and von Jagow [4] as the inhibitory site which inhibits by blocking a proton channel. The zinc is 10 Å from both the binding site of stigmatellin and the carboxylate of E272, and may involve residues which could contribute to a H-bonded path from the Q_o site to the aqueous phase. The existence of such an H-bonded network leading from the area of E272 and the heme propionates has been proposed based on low resolution structures [18,19], and has been visualized crystallographically [20]. In the latter case the network involves residues corresponding to R81 and N256, in the vicinity of the Zn01-binding site. It is possible that the Zinc reduces the rate of proton transfer to the bulk phase, thus inhibiting but not completely blocking turnover.

As shown in Fig. 1, the inhibitory site of the chicken enzyme has a lower affinity for Zn than that of the beef enzyme. This could be because the same site has lower affinity in the chicken enzyme, or because the beef inhibitory site is absent in chicken and inhibition is by a different site with lower affinity. Of the four likely ligands for Zn01, only residue E255 is different in the beef sequence. It is replaced by aspartate which because of its shorter side chain would probably not be able to ligate Zn01, and thus there is no reason to expect this site to have a higher affinity in the beef enzyme.

When refined assuming full occupancy, Zn01 and its potential ligands have B-factors around 112, indicating a high degree of disorder (This B-factor corresponds to a RMS displacement of the atoms of 1.2 Å). Due to close correlation of B-factor and occupancy when refined against low resolution data, we cannot say whether part of this is due to incomplete occupancy rather than disorder. However if this is the site with a binding constant around 3 μM, it should be nearly fully occupied at the concentration in the crystal (100–200 μM Zn). The B-factors for the side chains of D253, E255 and H121 are around 90, while H268 is also around 110.

Zn02 is another potential inhibitory site, as it binds in a channel where the tail of ubiquinol is presumed to bind, and through which the head of the quinone must pass to enter the site from the lipid phase of the membrane. The two residues in the vicinity of Zn01, M125 and F275 of cytochrome *b*, are the same in the beef enzyme. Mutually exclusive reversible binding of Zn and hydroquinone would be expected to lead to a competitive pattern of inhibition, which was not observed in the bovine complex, although competitive inhibition by Cu^{2+} was observed in the cytochrome b_6f complex [5]. Preliminary experiments with the chicken enzyme suggest non-competitive inhibition. The B-factors for Zn02 in the two monomers are similar to those of main-chain atoms in the transmembrane helices, so it is likely that these sites are fully occupied. However, a significant rate of turnover was observed with the chicken enzyme at similar concentrations. While there seems to be no room in the channel for quinol to enter and quinone to leave while Zn02 is present, we cannot rule out flexibility of the protein allowing some access. Another explanation could be that binding at this hydrophobic site in the membrane is very slow, and the site is not significantly occupied on the time scale of the inhibition assays.

Future work will include crystallographic studies of Zn binding in the beef $P6_522$ crystals, and pH and time dependence of inhibition and binding-site occupancy in the chicken enzyme. If it can be shown that inhibition is due to binding of Zn01, this will support a role for these residues in proton conduction. Absence of a Zn-binding site in subunit 2 makes it unlikely that the core proteins have a processing peptidase role, even for a single turnover to process the Rieske protein in the same complex.

Acknowledgements

This work was funded by NIH Grant R01DK44842 to E.A.B. This work was carried out at Lawrence Berkeley National Laboratory (LBNL) and Stanford Synchrotron Radiation Laboratory (SSRL). LBNL is supported by the Director, Office of Science, Office of Basic Energy Sciences, of the US Department of Energy under Contract No. DE-AC03-76SF00098. SSRL is operated by the Department of Energy, Office of Basic Energy Sciences. The SSRL Biotechnology Program is supported by the National Institutes of Health, National Center for Research Resources, Biomedical Technology Program, and by the Department of Energy, Office of Biological and Environmental Research.

References

[1] G. von Jagow, T.A. Link, Methods Enzymol. 126 (1986) 253–271.
[2] V.P. Skulachev, V.V. Chistyakov, A.A. Jasaitis, E.G. Smirnova, Biochem. Biophys. Res. Commun. 26 (1967) 1–6.
[3] M. Lorusso, T. Cocco, A.M. Sardanelli, M. Minuto, F. Bonomi, S. Papa, Eur. J. Biochem. 197 (1991) 555–561.
[4] T.A. Link, G. von Jagow, J. Biol. Chem. 270 (1995) 25001–25006.
[5] S. RaoBK, A. Tyryshkin, A. Roberts, M. Bowman, D. Kramer, Biochemistry 39 (2000) 3285–3296.
[6] U. Schulte, M. Arretz, H. Schneider, M. Tropschug, E. Wachter, W. Neupert, H. Weiss, Nature 339 (1989) 147–149.
[7] S. Gencic, H. Schagger, G. von Jagow, Eur. J. Biochem. 199 (1991) 123–131.
[8] N.D. Rawlings, A.J. Barrett, Biochem. J. 275 (1991) 389–391.
[9] S. Brumme, V. Kruft, U.K. Schmitz, H.P. Braun, J. Biol. Chem. 273 (1998) 13143–13149.
[10] E. Glaser, A. Eriksson, S. Sjoling, FEBS Lett. 346 (1994) 83–87.
[11] K. Deng, L. Zhang, A.M. Kachurin, L. Yu, D. Xia, H. Kim, J. Deisenhofer, C.A. Yu, J. Biol. Chem. 273 (1998) 20752–20757.
[12] D. Xia, C.A. Yu, H. Kim, J.Z. Xia, A.M. Kachurin, L. Zhang, L. Yu, J. Deisenhofer, Science 277 (1997) 60–66.
[13] Z. Zhang, L. Huang, V.M. Shulmeister, Y.I. Chi, K.K. Kim, L.W. Hung, A.R. Crofts, E.A. Berry, S.H. Kim, Nature 392 (1998) 677–684.
[14] S. Iwata, J.W. Lee, K. Okada, J.K. Lee, M. Iwata, B. Rasmussen, T.A. Link, S. Ramaswamy, B.K. Jap, Science 281 (1998) 64–71.
[15] B.L. Trumpower, C.A. Edwards, J. Biol. Chem. 254 (1979) 8697–8706.
[16] A.T. Brunger, P.D. Adams, G.M. Clore, W.L. DeLano, P. Gros, R.W. Grosse-Kunstleve, J.S. Jiang, J. Kuszewski, M. Nilges, N.S. Pannu, R.J. Read, L.M. Rice, T. Simonson, G.L. Warren, Acta Crystallogr. D 54 (1998) 905–921.
[17] I.L. Alberts, K. Nadassy, S.J. Wodak, Protein Sci. 7 (1998) 1700–1716.
[18] S. Izrailev, A.R. Crofts, E.A. Berry, K. Schulten, Biophys. J. 77 (1999) 1753–6178.
[19] A.R. Crofts, S. Hong, N. Ugulava, B. Barquera, R. Gennis, M. Guergova-Kuras, E.A. Berry, Proc. Natl. Acad. Sci. USA 96 (1999) 10021–10026.
[20] C. Hunte, J. Koepke, C. Lange, T. Roßmanith, H. Michel, Structure 8 (2000) 669–684.
[21] P.J. Kraulis, J. Appl. Crystallogr. 24 (1991) 946–950.
[22] E.A. Merrit, M.E.P. Murphy, Acta Crystallogr. D50 (1994) 869–873.
[23] T.A. Jones, J.-Y. Zhou, S.W. Cowan, M. Kjeldgaard, Acta Crystallogr. A47 (1991) 110–119.